



## Generation of the active Pd cluster catalyst in the Suzuki–Miyaura reactions: Effect of the activation with H<sub>2</sub> studied by means of quick XAFS

Kazu Okumura<sup>a,\*</sup>, Hirosuke Matsui<sup>a</sup>, Takashi Sanada<sup>a,b</sup>, Masazumi Arai<sup>b</sup>, Tetsuo Honma<sup>c</sup>, Sayaka Hirayama<sup>c</sup>, Miki Niwa<sup>a</sup>

<sup>a</sup> Department of Chemistry and Biotechnology, Graduate School of Engineering, Tottori University, Tottori 680-8552, Japan

<sup>b</sup> Research Department, NISSAN ARC, LTD., Yokosuka 237-0061, Japan

<sup>c</sup> Japan Synchrotron Radiation Research Institute, Hyogo 679-5198, Japan

### ARTICLE INFO

#### Article history:

Received 22 January 2009

Revised 3 April 2009

Accepted 21 April 2009

Available online 23 May 2009

#### Keywords:

Palladium

USY zeolite

Quick XAFS

Suzuki–Miyaura reaction

In situ activation

### ABSTRACT

Formation processes of the Pd clusters supported on USY were analyzed by means of time-resolved Quick XAFS. We found that the kind of precursors had profound effect on the formation of Pd<sup>0</sup> clusters. That is to say, Pd clusters with ca. 13 atoms were obtained through the addition of H<sub>2</sub> to Pd(NH<sub>3</sub>)<sub>4</sub>Cl<sub>2</sub>/USY at room temperature, where the partial pressure of H<sub>2</sub> hardly affected the size and the rate of formation of Pd clusters. In contrast, severe aggregation occurred over PdCl<sub>2</sub> and Pd(OAc)<sub>2</sub> loaded on USY. The Pd species generated on USY exhibited prominent activity in Suzuki–Miyaura reactions. The use of ammine complexes was indispensable to achieve high activity, in agreement with the Quick XAFS observations. The in situ activation (H<sub>2</sub> bubbling) was remarkably effective to activate the Pd/USY catalyst. These results represented that many factors including support, Pd precursor, and activation methods had profound effect on the genesis and the catalysis of Pd clusters.

© 2009 Elsevier Inc. All rights reserved.

### 1. Introduction

Metal clusters have been of particular concern due to their characteristics in versatile catalytic reactions [1,2]. Among the noble metals, Pd clusters have been the subject of extensive research because of its unique activities in various fine chemical syntheses such as Suzuki–Miyaura, Mizoroki–Heck, and Sonogashira cross-coupling reactions [3]. Recently, we found that metal Pd clusters could be readily obtained on Pd/USY through the exposure of H<sub>2</sub> at room temperature [4]. Furthermore, the size of the Pd clusters was readily controlled by changing the number of times for the iterative introduction of H<sub>2</sub> and O<sub>2</sub> flows to the Pd/USY as illustrated in Fig. 1. In this study, reduction of Pd<sup>2+</sup> and the growing processes of the Pd clusters were investigated in detail by means of Quick XAFS (QXAFS). QXAFS technique is a powerful tool to study the dynamic structural changes of materials. Unlike the usual step-scan method, the monochromator is continuously moved in the quick mode. Using this technique, it is possible to collect data in a short time and to detect the changes in the structure easily under in situ conditions. The powerful X-ray source in SPring-8 with a high photon flux of 10<sup>9</sup>–10<sup>11</sup> photons s<sup>-1</sup> enabled us to detect minute changes in the Pd structure in the zeolite pores [5,6]. In addition, the fact that X-ray absorption in zeolite matrix is

small in comparison to that in Pd at the energy region of the Pd-K edge (24.3 keV) is suitable to collect high-quality data even for low Pd-loadings such as 0.4 wt%. Here, the QXAFS data were correlated with the catalytic performance of Pd/USY in the Suzuki–Miyaura cross-coupling reaction. This reaction has been extensively studied and has become one of the most efficient methods for the C–C bond formation using phenylboronic acid derivatives and halogenated aryls [7,8]. Till date, numerous Pd complexes including bulky phosphines [9,10], *N*-heterocyclic carbenes [11,12], and palladacycles [13,14] have been applied to Suzuki–Miyaura reactions. Moreover, very high activity was achieved under particular conditions; Leadbeater found surprisingly a high turn-over number (TON) in the Suzuki–Miyaura coupling using microwave heating [15]. Reetz reported that the ammonium salt-stabilized Pd or polymer-stabilized Pd clusters were active in the phosphine-free Suzuki–Miyaura and Heck reactions [16]. On the other hand, supported Pd catalysts are considered as another candidate for Suzuki–Miyaura reactions. They are readily prepared and rather inexpensive. In addition, they are easily separated from the product after the reaction. For this purpose, Pd has been supported on various types of supports including active carbon [17,18], zeolites [19,20], layered double hydroxide [21], modified silica [22], hydroxyapatite [23], and polymers such as dendrimers and polyethylene glycol [24,25]. However, in general, the catalytic activity of heterogeneous catalysts is lower than that of homogeneous catalysts. In this regard, zeolites are promising supports for Pd due to their large

\* Corresponding author. Fax: +81 857 31 5684.

E-mail address: [okmr@chem.tottori-u.ac.jp](mailto:okmr@chem.tottori-u.ac.jp) (K. Okumura).

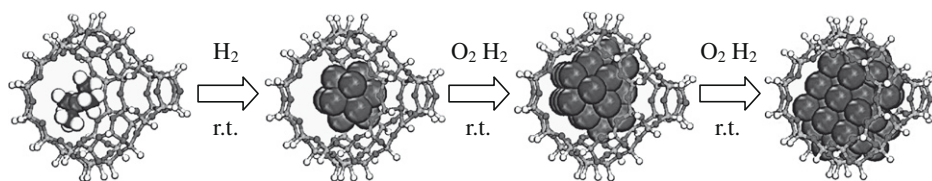


Fig. 1. Stepwise growth of Pd clusters in the supercage of USY zeolite.

surface area and the existence of uniform micropores to accommodate dispersed metal clusters that lead to a high surface-to-volume ratio. Indeed, Okitsu et al. synthesized Pd nano-clusters on NaY zeolite via a sonochemical process [26]. Moreover, well-dispersed metal clusters having surface atoms with low coordination number (CN) are expected to exhibit a high activity; this behavior is different from that of the bulk-type catalyst. As a matter of fact, Artok et al. recently reported that Pd<sup>2+</sup> or Pd<sup>0</sup> clusters loaded on the NaY zeolite were efficient in the Suzuki–Miyaura reactions using various substrates [20,27]. Jacobs et al. reported that the Pd(NH<sub>3</sub>)<sub>4</sub><sup>2+</sup>-zeolites and Pd<sup>0</sup>-mordenite are not only active and selective but also truly heterogeneous catalysts in the Heck reactions [28]. Djakovitch and Köhler found that Palladium-complex-loaded Na–Y zeolites exhibit a high activity towards the Heck reaction of aryl bromides with olefins [29]. These studies stimulated us to further improve the catalytic performance of the Pd/FAU-zeolite catalyst by choosing appropriate conditions for the pre-treatment to afford the active Pd<sup>0</sup> clusters, which was predicted by the QXAFS data measured under in situ conditions.

## 2. Experimental

### 2.1. Sample preparations

NH<sub>4</sub>–USY (HSZ–341NHA, Si/Al<sub>2</sub> = 7.7) zeolite was supplied by Tosoh Co. The NH<sub>4</sub>–USY was transformed to the H<sup>+</sup>-form through the thermal treatment at 773 K in a N<sub>2</sub> flow. An ion-exchange method using a Pd(NH<sub>3</sub>)<sub>4</sub>Cl<sub>2</sub> solution (3.8 × 10<sup>−4</sup> mol dm<sup>−3</sup>, Aldrich) was used to load Pd on the USY. The ion-exchange procedure was carried out at r.t. for 12 h. The samples were thoroughly washed with water, followed by drying in an oven maintained at 323 K under atmospheric conditions. The loading of Pd was measured by inductively coupled plasma (ICP) after the ion-exchange procedures. The typical loading of Pd was 0.4 wt%. PdCl<sub>2</sub>, Pd(OAc)<sub>2</sub>, and Pd(NH<sub>3</sub>)<sub>4</sub>(NO<sub>3</sub>)<sub>2</sub> (Wako Chemicals) were supported on USY with the loading of 0.4 wt% in a similar manner for the preparation of Pd(NH<sub>3</sub>)<sub>4</sub>Cl<sub>2</sub>/USY. As an exception, toluene was used as the solvent for the preparation of Pd(OAc)<sub>2</sub>/USY, instead of water. Pd(NH<sub>3</sub>)<sub>4</sub>Cl<sub>2</sub> was also loaded on Na–Y (Si/Al<sub>2</sub> = 5.5, HSZ–320NAA, Tosoh Co.), ZSM-5 (HSZ–840HOA, Si/Al<sub>2</sub> = 40, Tosoh Co.), and Mordenite (JRC-Z-M20, Si/Al<sub>2</sub> = 20, Catalysis Society of Japan) in an analogous way for the preparation of Pd(NH<sub>3</sub>)<sub>4</sub>Cl<sub>2</sub>/USY. Pd (0.4 wt%) loaded on Al<sub>2</sub>O<sub>3</sub> (JRC-ALO-3, Catalysis Society of Japan) and active carbon (Wako Chemicals Co.) were prepared by the impregnation method using a Pd(NH<sub>3</sub>)<sub>4</sub>Cl<sub>2</sub> solution.

### 2.2. Quick XAFS measurements and analysis

Synchrotron radiation experiments were carried out at the BL14B2 and BL01B1 stations with the approval of the Japan Synchrotron Radiation Research Institute (JASRI/SPring-8) (Proposal No. 2007A1417, No. 2008B1237). XAFS data were collected in a quick mode; that is to say, the Si(111) monochromator was continuously moved from 4.72° to 4.45° in 36 s (0.6 m). In the in situ measurement, a wafer form of the sample was placed in a quartz cell. The thickness of the sample was adjusted to be 1.5 cm in order

to provide edge jumps of 0.3. Time-resolved QXAFS measurements were carried out at r.t. (300 K) in a flow of 0.6–50% H<sub>2</sub>; helium was used as the balance gas. The total flow rate for H<sub>2</sub>/He was 90 ml min<sup>−1</sup>. For the temperature-programmed measurements, the sample placed in the cell was heated from r.t. to 773 K with a ramp rate of 5 K min<sup>−1</sup> in an 8%–H<sub>2</sub>/He flow (total flow rate, 90 ml min<sup>−1</sup>) at atmospheric pressure. For the EXAFS analysis, the oscillations were extracted by a spline smoothing method. The Fourier transformation of the k<sup>3</sup>-weighted EXAFS oscillations, k<sup>3</sup>χ(k), from k space to r space was performed over a range of 30–130 nm<sup>−1</sup> to obtain a radial distribution function. The inversely Fourier-filtered data were analyzed using a curve-fitting method in the k range between 30 and 130 nm<sup>−1</sup> [30]. For the analysis of the spectra obtained in the temperature-programmed measurements, the Debye–Waller factors of Pd–N(O) and the nearest-neighboring Pd–Pd bond were extracted from the spectra of PdO and Pd foil, respectively, at the same temperatures as those of the experimental samples. The parameters extracted from PdO were utilized for calculation of the Pd–N bond as well. This is because it is generally assumed that the phase shifts and backscattering amplitudes are transferable among the nearest neighbors in the periodic table. Curve-fitting analysis was initiated by employing the extracted Debye–Waller factors. The inversely Fourier-filtered data were analyzed by a usual curve-fitting method based on Eq. (1)

$$\chi(k) = \sum N_j F_j(k) \exp(-2\sigma_j^2 k_j^2) \sin(2kr_j + \phi_j(k)) / kr_j^2 \quad (1)$$

$$k_j = (k^2 - 2m\Delta E_{0j}/\hbar^2)^{1/2}$$

where  $N_j$ ,  $r_j$ ,  $\sigma_j$ , and  $\Delta E_{0j}$  represent the coordination number, the bond distance, the Debye–Waller factor, and the difference in the threshold energy between reference and sample, respectively. The degree of error bars in the present curve-fitting analysis for  $\Delta E_{0j}$  and  $\sigma_j$  is estimated to be 4 eV and 0.002 nm, respectively.  $F_j(k)$  and  $\phi_j(k)$  represent amplitude and phase shift functions, respectively. The analysis of the EXAFS data was performed using the REX2000 (ver. 2.0.4) program produced by RIGAKU Ltd.

### 2.3. Transmission electron microscope observation of Pd/USY reduced with H<sub>2</sub>

In order to check the dispersion of Pd over the USY support, the transmission electron microscope (TEM) images were taken by means of a HITACHI H-9000UHR microscope with an acceleration voltage of 300 kV. The specimen for TEM observation was prepared by crushing method and the observations were carried out at r.t.

### 2.4. Catalytic reactions

Pd-loaded samples were treated with a H<sub>2</sub> flow by the in situ activation method (bubbling); a 6%–H<sub>2</sub>/94%–Ar flow with the rate of 30 ml min<sup>−1</sup> was fed into the reactant solution using a capillary glass tube at r.t. In the typical condition, bromobenzene (7.85 g, 50 mmol), phenylboronic acid (9.75 g, 80 mmol), K<sub>2</sub>CO<sub>3</sub> (13.8 g, 100 mmol), tridecane (internal standard, 8.1 g), and the catalyst (1.0 mg, 3.8 × 10<sup>−8</sup> mol Pd) were used for Suzuki–Miyaura reactions. The reaction was carried out in 140 mL of *o*-xylene as a sol-

vent. In the reaction, phenylboronic acid,  $K_2CO_3$ , the catalyst, bromobenzene, and tridecane were placed in the flask prior to the addition of *o*-xylene. The scales of whole reagents were varied, while the catalyst weight was fixed at 1.0 mg. Exceptionally,  $H_2O$ , *N,N*-dimethylformamide (DMF) and their mixture (1:1) were used as the solvents for reactions. The three-necked flask was placed in a pre-heated oil bath at 383 K (solvent: *o*-xylene, and DMF) or 373 K (solvent:  $H_2O$  and DMF/ $H_2O$ ) in an atmosphere of  $N_2$  with vigorous stirring. After the reaction, the reaction mixture was cooled to r.t., and then the solution was analyzed with the Shimadzu 2010 Gas Chromatograph equipped with the MDN-12 or TC-17 (30 m) capillary column. In the analysis, tridecane or tetradecane was used as an internal standard. For the reaction using  $H_2O$  as the solvent, the solution was extracted with ethyl acetate. The extract was analyzed by GC after drying over  $MgSO_4$ .

### 3. Results and discussion

#### 3.1. QXAFS analysis on the formation process of Pd clusters in Pd/USY

First, QXAFS technique was applied to collect the Pd-K edge EXAFS data of Pd/USY, which was prepared from  $Pd(NH_3)_4Cl_2$  as the precursor. Fig. 2a shows the Pd-K edge EXAFS Fourier transforms of 0.4 wt%-Pd/USY measured every 0.6 min in 5%- $H_2$  atmosphere at r.t. (300 K). The Pd–N bond can be seen at 0.16 nm in the initial state. On exposure to  $H_2$ , the Pd–N ( $NH_3$  ligand) bond quickly disappeared, while the metal Pd–Pd bond emerged at 0.25 nm (phase shift uncorrected), thereby, indicating that  $Pd^{2+}$  was reduced to  $Pd^0$  in 20 min. Fig. 2b shows the change in the CN plotted as a function of duration time. The reduction of  $Pd^{2+}$  and the alternative growth of  $Pd^0$  completed up to 20 min. At this point, CN of the Pd–Pd bond was calculated to be 5.2, which was close to the CN of  $Pd_{13}$  clusters with a cuboctahedron structure (CN = 5.5). The Pd clusters were stable up to 443 K as reported already [4]. Then, the formation of the Pd clusters was followed in an atmosphere of  $H_2$  with different partial pressures in order to obtain an insight into the formation process of Pd clusters. Fig. 3 shows the Pd-K edge EXAFS data of Pd clusters generated under  $H_2$  with different partial pressures. The measurement was carried out after 30 min from the introduction of  $H_2$ , when the reduction of  $Pd^{2+}$  was completed. It was evident that the peak height of the Pd–Pd bond was much lower than that of Pd foil. In addition, unlike the spectrum of Pd foil, no peak longer than 0.4 nm was observed, indicating the formation of small Pd clusters. The parameters obtained by the structural analysis are given in Table 1. It can be seen that the structural parameters of Pd clusters are practically the same, meaning that the change in the partial pressure of  $H_2$  over 0.6–50% did not affect the structure of Pd clusters. The distance of the nearest-neighbor Pd–Pd bond of these clusters was slightly longer than that of Pd foil, implying the absorption of H into the clusters. Then, the change in the valence state of Pd was followed by the analysis of XANES region. Fig. 4 shows the example of Pd-K edge XANES of Pd/USY measured every 0.6 min at 300 K. In the initial stage, the spectrum of Pd/USY was similar to that of  $Pd(NH_3)_4Cl_2$ . The XANES shape gradually changed with duration of time; eventually the spectra became similar to that of Pd foil. In order to determine the relative concentrations of metal  $Pd^0$  and  $Pd^{2+}$  in the course of the reduction with  $H_2$ , the XANES were fitted by the combination of the spectra for Pd/USY collected before and after the completion of the reduction of Pd using a least-square method. In other words, the spectra obtained before the introduction of  $H_2$  and that obtained after exposure to  $H_2$  for 30 min, at which the reduction of Pd was completed, were employed for the calculation of the spectra [4]. The oxidation state of Pd was kinetically analyzed based on the data given in Fig. 4. That is, the change in the concentration of

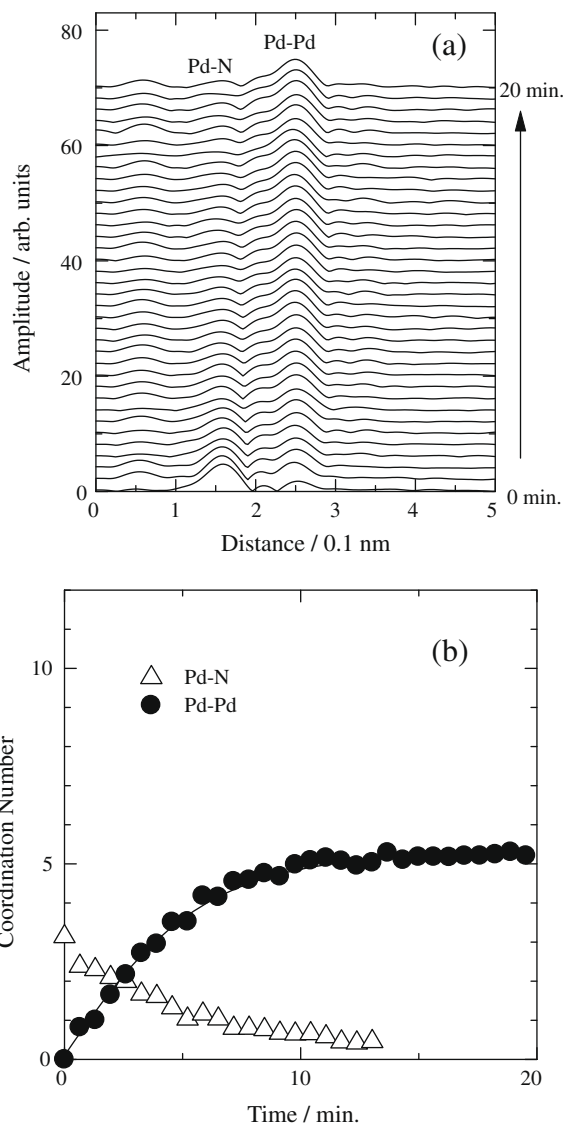


Fig. 2. (a) Pd-K edge EXAFS Fourier transforms of 0.4 wt%- $Pd(NH_3)_4Cl_2/USY$  measured in the atmosphere of 5%  $H_2$  at 300 K and (b) coordination numbers of the Pd–N ( $\Delta$ ) and nearest-neighbor Pd–Pd ( $\bullet$ ) bond.

$Pd^{2+}$  cations determined from XANES was analyzed assuming the first-order reaction kinetics; the value of  $\ln(C_0/C)$  (where  $C$  represents the concentration of  $Pd^{2+}$ ) was plotted as a function of time (Fig. 5a). As can be seen in the figure, a linear correlation between  $\ln(C_0/C)$  and time was obtained. The first-order rate constant,  $k$ , was plotted with log scales as a function of partial pressure of  $H_2$  (Fig. 5b). The slope of the relationship was calculated to be 0.08, meaning the partial pressure of  $H_2$  hardly affected the reduction rate of  $Pd^{2+}$ .

#### 3.2. Formation processes of $Pd^0$ over Pd/USY prepared with various Pd sources

The reduction process of Pd was followed by QXAFS using Pd/USY samples prepared with different kinds of Pd sources. Fig. 6a shows Pd-K edge EXAFS Fourier transforms of 0.4 wt%- $PdCl_2/USY$  measured in a flow of 5%  $H_2$  at r.t. A peak can be seen at 0.18 nm before exposure to  $H_2$  (0 min), which was assignable to the Pd–Cl bond from the comparison with the spectrum of unsupported  $PdCl_2$ . After the admission of  $H_2$ , the intensity of the Pd–Cl bond

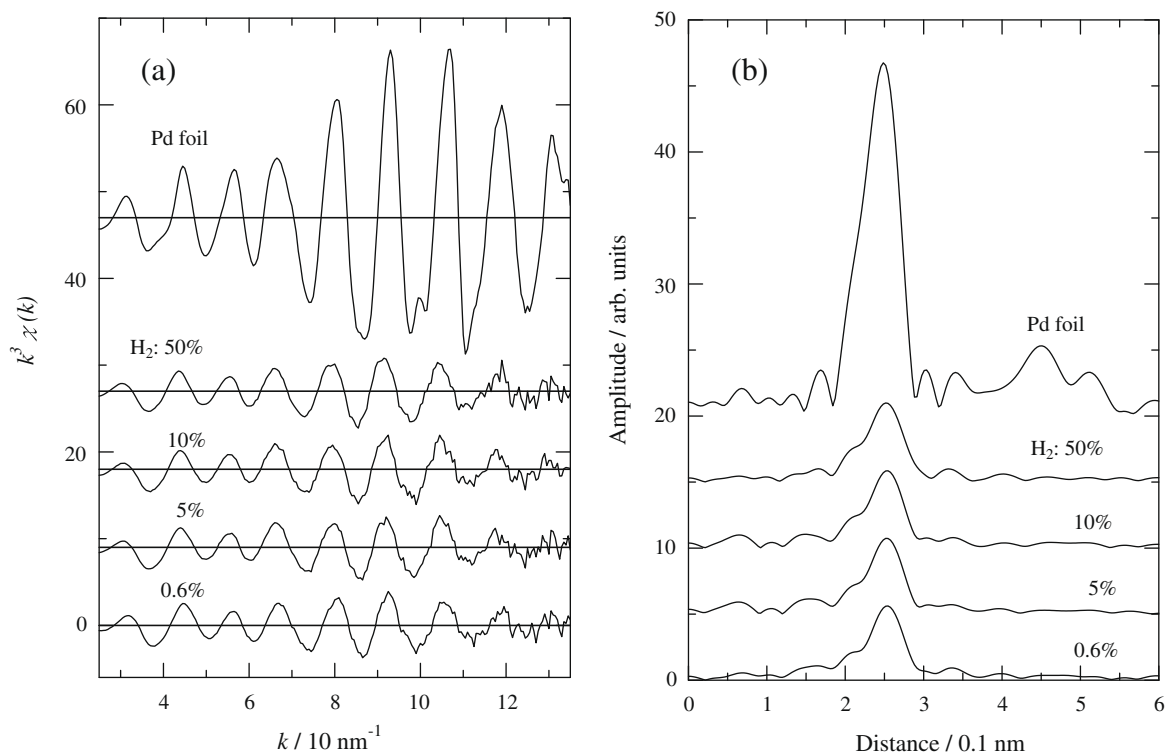


Fig. 3. Pd-K edge EXAFS (a)  $k^3\chi(k)$  and (b) their Fourier transforms of 0.4 wt%-Pd(NH<sub>3</sub>)<sub>4</sub>Cl<sub>2</sub>/USY reduced with 0.6–50% H<sub>2</sub> diluted with He at 300 K for 30 min.

Table 1

Curve-fitting analysis of Pd-K edge EXAFS data measured at r.t. for 0.4 wt%-Pd/USY after the treatments with H<sub>2</sub>.

H <sub>2</sub> (%) <sup>a</sup>	Scatter	CN <sup>b</sup>	R (nm) <sup>c</sup>	$\Delta E_0$ (eV) <sup>d</sup>	DW (nm) <sup>e</sup>	R <sub>f</sub> (%) <sup>f</sup>
0.6	Pd	5.8 ± 0.2	0.275 ± 0.001	3	0.009	0.7
5	Pd	5.5 ± 0.2	0.276 ± 0.001	2	0.009	0.6
10	Pd	5.7 ± 0.2	0.277 ± 0.001	2	0.009	0.7
50	Pd	5.9 ± 0.2	0.277 ± 0.001	1	0.009	0.5
(Pd foil) <sup>g</sup>	Pd	12	0.274			

<sup>a</sup> Partial pressure of H<sub>2</sub>.

<sup>b</sup> Coordination number.

<sup>c</sup> Bond distance.

<sup>d</sup> Difference in the origin of photoelectron energy between the reference and the sample.

<sup>e</sup> Debye–Waller factor.

<sup>f</sup> Residual factor.

<sup>g</sup> Data of X-ray crystallography. Fourier transform range: 30–130 nm<sup>-1</sup>. Fourier filtering range: 0.17–0.32 nm.

rapidly decreased in less than 2 min. Alternatively, the Pd–Pd bond assignable to the metal Pd<sup>0</sup> emerged at 0.26 nm (phase shift uncorrected). Fig. 6b shows the change in the CNs of Pd–Cl and Pd–Pd bonds. The Pd–Cl completely diminished at 2 min. At this stage, the CN of Pd–Pd bond already reached to 10.5. The particle size of Pd<sup>0</sup> could be estimated to be ca. 3 nm on the basis of the CN value. The fact suggested that the severe aggregation occurred when PdCl<sub>2</sub> was used for the preparation of Pd/USY.

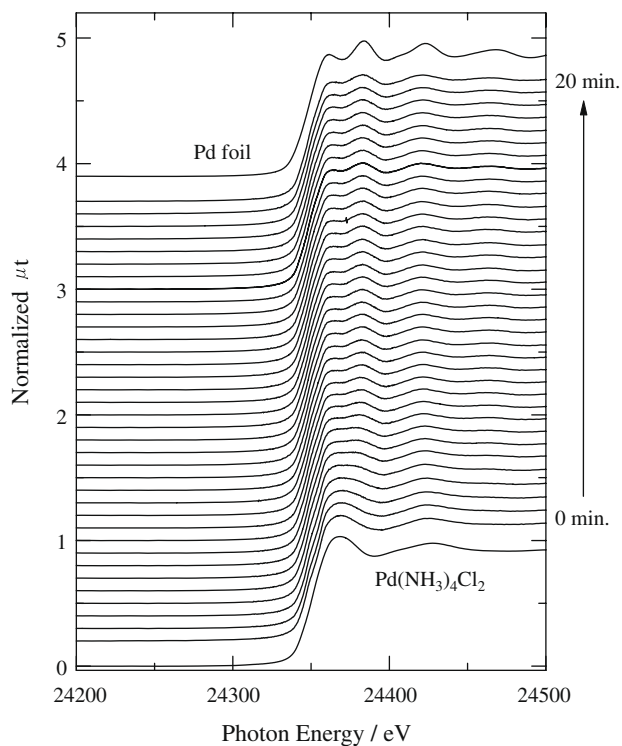
Fig. 7 shows the Pd-K edge EXAFS Fourier transforms and their curve-fitting results of 0.4 wt%-Pd(OAc)<sub>2</sub>/USY measured in a flow of 8% H<sub>2</sub> during temperature-programmed heating. In this case, the reduction of Pd<sup>2+</sup> was incomplete at r.t. On raising the temperature, the CN of Pd–Pd bond continued to increase even after the disappearance of Pd–O bond, meaning that the stable Pd clusters were not obtained with the use of Pd(OAc)<sub>2</sub> as a precursor, similarly to the case of PdCl<sub>2</sub>/USY.

Fig. 8 shows the Pd-K edge EXAFS Fourier transforms and their curve-fitting results of 0.4 wt%-Pd(NH<sub>3</sub>)<sub>2</sub>(NO<sub>3</sub>)<sub>2</sub>/USY measured in a flow of 8% H<sub>2</sub> during temperature-programmed heating. Unlike

the case for Pd/USY prepared from Pd(NH<sub>3</sub>)<sub>2</sub>Cl<sub>2</sub>, the Pd<sup>2+</sup> was not reduced at r.t. Accompanied by an increase in the temperature, Pd<sup>2+</sup> was completely reduced at 363 K as was confirmed from the disappearance of the Pd–N bond. At this point, the CN of Pd–Pd bond (Pd<sup>0</sup>) reached 5.0. The CN kept constant value up to 403 K. Subsequently, the CN(Pd–Pd) rapidly increased on further raising the temperature, meaning the aggregation of Pd progressed. The appearance of the plateau in the temperature range between 363 and 403 K meant the formation of the meta-stable Pd clusters at this temperature range. It should be noted that the CN = 5.0 was close to that of the Pd clusters generated on Pd(NH<sub>3</sub>)<sub>4</sub>Cl<sub>2</sub>/USY. The above data indicated that the use of Pd ammine complexes was essential to give rise to the formation of Pd clusters on the support of USY.

### 3.3. The TEM image of Pd/USY reduced with H<sub>2</sub>

We show the TEM lattice image of Pd/USY reduced with 6% H<sub>2</sub> for 30 min at r.t. in Fig. 9, as an example of our observation results.



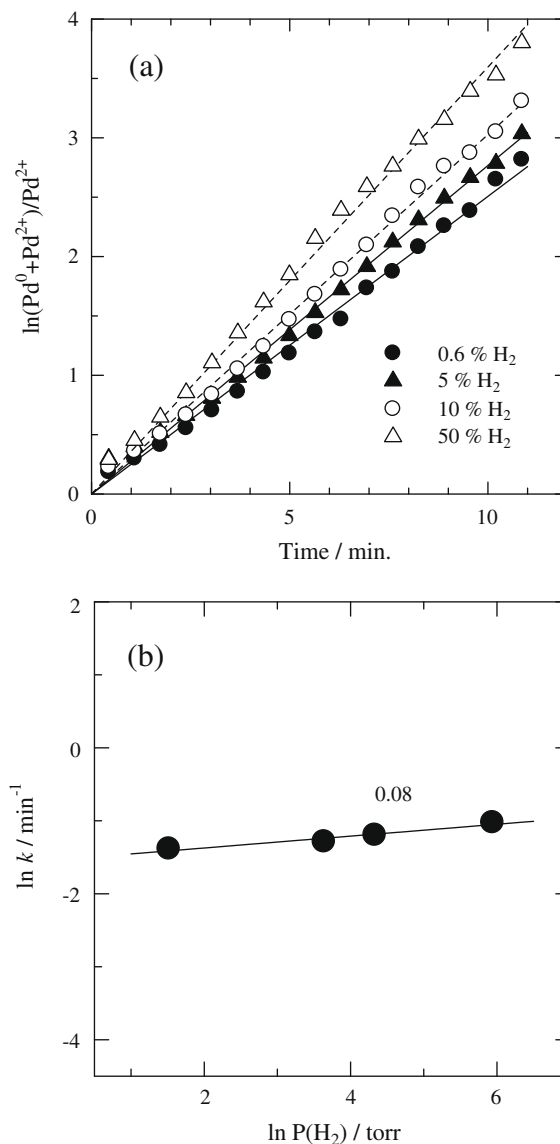
**Fig. 4.** Pd-K edge XANES of 0.4 wt%-Pd(NH<sub>3</sub>)<sub>4</sub>Cl<sub>2</sub>/USY measured every 0.6 min in a 5% H<sub>2</sub> flow.

Although the lattice fringe of the USY support was visible, Pd particle was not found even at the magnification of  $\times 1,600,000$ , presumably due to the formation of finely dispersed Pd clusters as expected from the QXAFS data.

#### 3.4. Effect of the pre-treatment conditions and the selection of support on the catalytic performance of Pd/USY

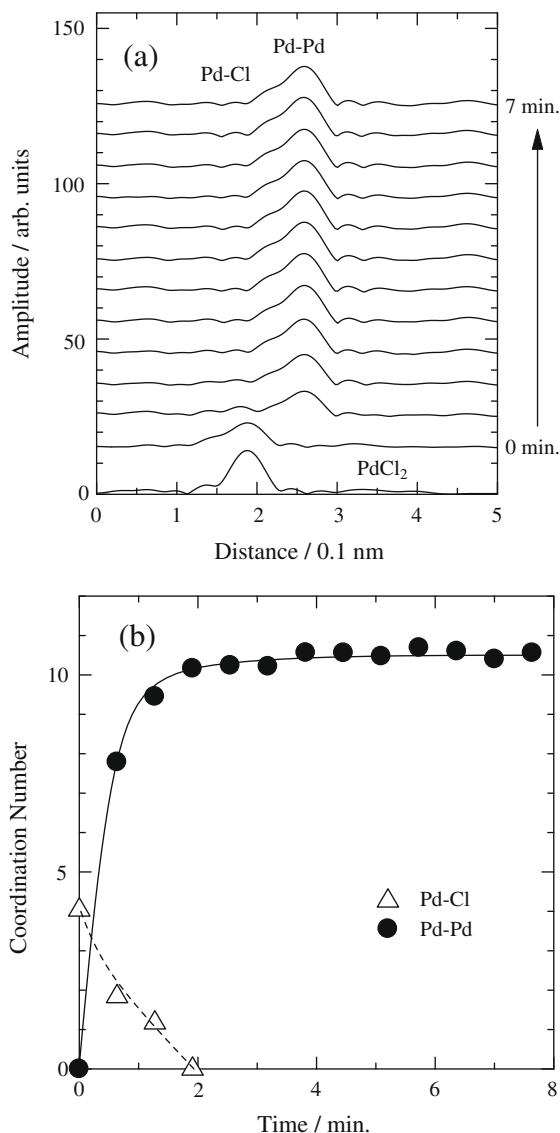
Then Suzuki–Miyaura coupling reactions were carried out over Pd clusters fabricated on the USY support. Pd(NH<sub>3</sub>)<sub>4</sub>Cl<sub>2</sub> was employed for the preparation of the catalyst. In order to obtain Pd clusters under in situ conditions, the bubbling method was applied to form Pd clusters, that is, a 6% H<sub>2</sub> flow at the rate of 30 mL min<sup>-1</sup> was fed into the reactant solution using a capillary glass tube at r.t. The H<sub>2</sub> flow continued for 30 min. After this, the formation of Pd clusters might be completed as can be seen in the QXAFS data (Fig. 2). In a typical reaction condition, a small amount of 0.4 wt%-Pd/USY (1.0 mg) was used with respect to 50 mmol of bromobenzene that corresponds to 0.00007 mol%-Pd. As a result, we found that the Pd clusters generated under the in situ conditions worked very efficiently in Suzuki–Miyaura reactions. Fig. 10 shows typical time course change in the conversion of bromobenzene in the reaction with phenylboronic acid. In the case of Pd/USY activated with bubbling H<sub>2</sub>, the conversion of bromobenzene reached 56% in 5 min, and the reaction was completed in 2 h, wherein the TON of Pd reached 1,300,000. Although the high activity was also obtained on Pd/Na–Y, the intrinsic activity of Pd/Na–Y was slightly lower than that of Pd/USY.

Data on the Suzuki–Miyaura reaction between bromobenzene and phenylboronic acid over various catalysts and those catalysts activated with H<sub>2</sub> under various conditions are compared in Table 2. The Pd(NH<sub>3</sub>)<sub>4</sub>Cl<sub>2</sub>/USY activated by bubbling with 6% H<sub>2</sub> exhibited the highest TON among the tested catalysts, where TON = 1,300,000 (entry 4, yield = 100%) and TON = 1,700,000 (entry 5, yield = 64%) were attained as mentioned above. In contrast to the



**Fig. 5.** (a) Dependence of  $\ln(C_0/C)$  on the duration time measured in a H<sub>2</sub> flow. Catalyst: 0.4 wt%-Pd(NH<sub>3</sub>)<sub>4</sub>Cl<sub>2</sub>/USY. C represents the relative concentration of Pd<sup>2+</sup> determined from XANES analysis. (b) Dependence of the rate constant (*k*) for the reduction of Pd<sup>2+</sup> on the partial pressure of H<sub>2</sub>.

in situ-activated Pd/USY with H<sub>2</sub>, the as received Pd/USY (entry 1), Pd/USY treated with bubbling N<sub>2</sub> (entry 2), and Pd/USY reduced with 6% H<sub>2</sub> at 473 K (entry 3) exhibited much low TON less than 66,000. The reason for the negligible activity of the Pd/USY reduced at 473 K could probably be attributed to the formation of aggregated Pd, as expected from the QXAFS data reported earlier [4]. That is to say, the Pd clusters were no longer stable at 473 K. On the other hand, Pd-loaded on Al<sub>2</sub>O<sub>3</sub>, active carbon, ZSM-5, and Mordenite were subjected to the reaction after activation with bubbling H<sub>2</sub> in a manner similar to that for Pd/USY. The activities of these catalysts were much lower than that of Pd/USY; the highest TON value among these was obtained over Pd/Al<sub>2</sub>O<sub>3</sub> (entry 8, TON = 120,000). Although in situ activation was also effective for the Pd(OAc)<sub>2</sub> that worked in the homogenous phase, the activity (entry 14, TON = 370,000) was lower than that of Pd/USY activated with H<sub>2</sub> under in situ conditions (entry 5, TON = 1,700,000). From the striking difference in the catalytic performance between activation methods and the supports for Pd, specific nature of the

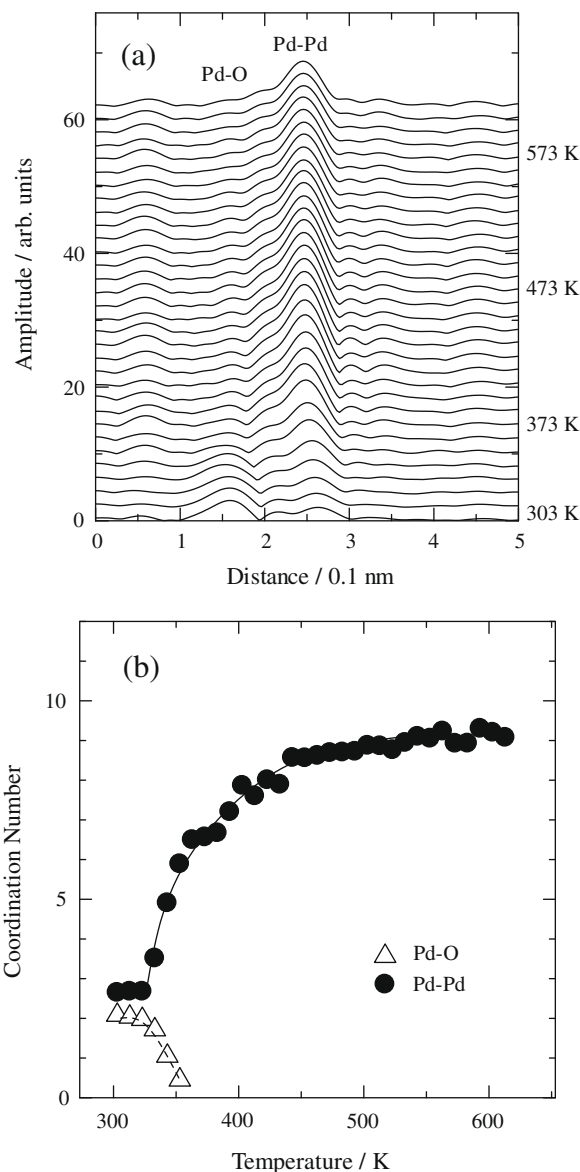


**Fig. 6.** (a)  $k^3$ -weighted Pd-K edge EXAFS Fourier transforms of 0.4 wt%-PdCl<sub>2</sub>/USY measured in an 8% H<sub>2</sub> flow at 300 K and PdCl<sub>2</sub> (Fourier transform range, 30–130 nm<sup>-1</sup>). (b) CNs of Pd-Pd (●) and Pd-Cl (Δ) bonds.

Pd/USY catalyst and the importance of in situ activation can be recognized.

### 3.5. Suzuki–Miyaura reactions using various kinds of substrates over Pd/USY activated with bubbling H<sub>2</sub>

The results of Suzuki–Miyaura reactions using various kinds of bromobenzene and phenylboronic acid derivatives over Pd/USY activated under in situ conditions are summarized in Table 3. High TONs up to 5,300,000 (entry 2) were obtained over various kinds of substances in a short time. In the case of 4-bromoacetophenone and phenylboronic acid as the reactants, the use of only 1.0 mg of Pd/USY afforded 40 g of product. The reaction using 4-bromoacetophenone proceeded even at r.t. (entry 18). These facts indicated the versatility of the in situ-activated Pd/USY in Suzuki–Miyaura reactions. The Pd/USY catalyst activated with bubbling H<sub>2</sub> is beneficial from the viewpoint of the simple preparation method and the low cost that is important in the industrial application, which could be realized by using a minimum amount of catalyst of 1.0 mg. Unfortunately, the repeated use of the in situ-

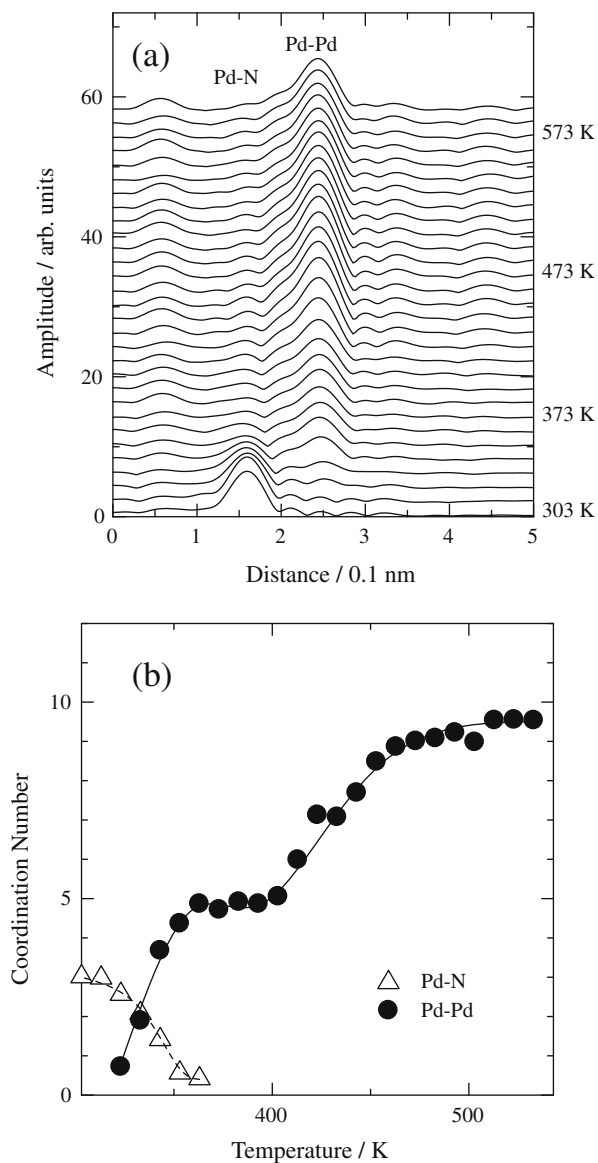


**Fig. 7.** (a)  $k^3$ -weighted Pd-K edge EXAFS Fourier transforms of 0.4 wt%-Pd(OAc)<sub>2</sub>/USY measured in the course of temperature-programmed reduction (Fourier transform range, 30–130 nm<sup>-1</sup>). (b) CNs of Pd-Pd (●) and Pd-O (Δ) bonds.

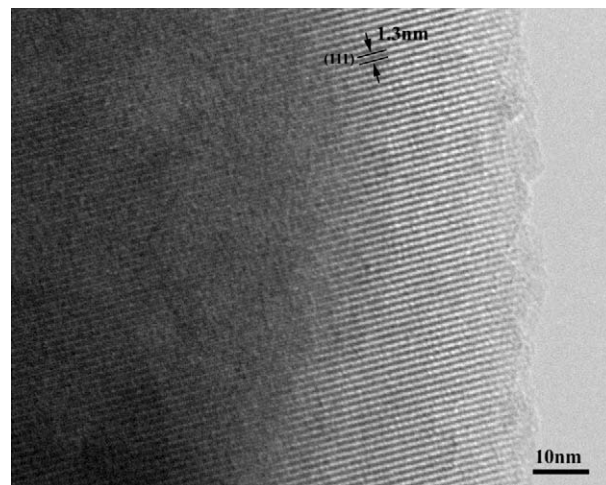
activated Pd/USY seemed to be difficult, taking into account the extremely small amount of the catalyst utilized for reactions (1.0 mg) and the instability of Pd clusters when it was exposed to air as expected from the QXAFS data. However, the very high TON obtained over Pd/USY seems to be more important than its recyclability for practical applications as pointed out by Gladysz [31].

### 3.6. Effect of the kinds of Pd sources

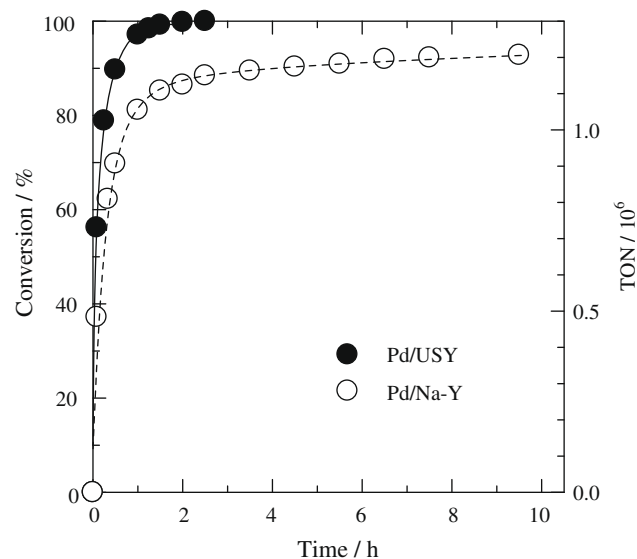
The results of Suzuki–Miyaura reaction (bromobenzene and phenylboronic acid) using Pd/USY prepared with various kinds of Pd precursors are given in Table 4. The in situ activation of Pd(NH<sub>3</sub>)<sub>4</sub>(NO<sub>3</sub>)<sub>2</sub>/USY was carried out at 373 K, taking into account the information obtained by QXAFS, that is, the formation of Pd clusters was observed in the temperature range between 363 and 403 K. The Pd/USY prepared from Pd ammine complexes, i.e. Pd(NH<sub>3</sub>)Cl<sub>2</sub> and Pd(NH<sub>3</sub>)<sub>4</sub>(NO<sub>3</sub>)<sub>2</sub>, exhibited very high activity (entries 1 and 2, TON = 1,700,000). In contrast to these, the Pd/USY catalysts prepared from Pd(OAc)<sub>2</sub> and PdCl<sub>2</sub> precursors exhibited



**Fig. 8.** (a)  $k^3$ -weighted Pd-K edge EXAFS Fourier transforms of 0.4 wt%-Pd(NH<sub>3</sub>)<sub>4</sub>(NO<sub>3</sub>)<sub>2</sub>/USY measured in the course of temperature-programmed reduction (Fourier transform range, 30–130 nm<sup>-1</sup>). (b) CNs of Pd-Pd (●) and Pd-N (△) bonds.



**Fig. 9.** The TEM image of 0.4 wt%-Pd(NH<sub>3</sub>)<sub>4</sub>Cl<sub>2</sub>/USY reduced with H<sub>2</sub> at 300 K.



**Fig. 10.** Time course change in the conversion of bromobenzene over 0.4 wt%-Pd(NH<sub>3</sub>)<sub>4</sub>Cl<sub>2</sub>/USY (●) and 0.4 wt%-Pd(NH<sub>3</sub>)<sub>4</sub>Cl<sub>2</sub>/Na-Y (○) activated with bubbling H<sub>2</sub>. Reaction conditions: bromobenzene (50 mmol), phenylboronic acid (80 mmol), catalyst (1.0 mg,  $3.8 \times 10^{-8}$  mol of Pd), K<sub>2</sub>CO<sub>3</sub> (100 mmol), *o*-xylene (140 mL), 383 K, N<sub>2</sub> atmosphere.

**Table 2**

Results of coupling reactions between bromobenzene and phenylboronic acid catalyzed by Pd-loaded catalysts activated under various conditions<sup>a</sup>.

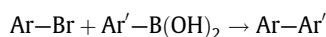
Entry	Catalyst	Activation method	Pd (10 <sup>-4</sup> mol%)	Time (h)	Yield (%)	TON
1 <sup>b</sup>	Pd/USY	As received	7.5	2.0	38	51,000
2 <sup>b</sup>	Pd/USY	N <sub>2</sub> , bubbling	7.5	2.0	45	66,000
3 <sup>b</sup>	Pd/USY	H <sub>2</sub> , 473 K	7.5	2.0	1	1000
4 <sup>b</sup>	Pd/USY	H <sub>2</sub> , bubbling	0.7	2.0	>99	1,300,000
5 <sup>b</sup>	Pd/USY	H <sub>2</sub> , bubbling	0.4	2.0	64	1,700,000
6 <sup>b</sup>	Pd/Na-Y	H <sub>2</sub> , bubbling	0.7	7.5	90	1,200,000
7 <sup>b</sup>	Pd/Al <sub>2</sub> O <sub>3</sub>	As received	7.5	2.0	30	40,000
8 <sup>b</sup>	Pd/Al <sub>2</sub> O <sub>3</sub>	H <sub>2</sub> , bubbling	7.5	2.0	92	120,000
9 <sup>b</sup>	Pd/Active Carbon	As received	7.5	2.0	11	14,000
10 <sup>b</sup>	Pd/Active Carbon	H <sub>2</sub> , bubbling	7.5	2.0	48	64,000
11 <sup>b</sup>	Pd/ZSM-5	H <sub>2</sub> , bubbling	7.5	1.0	1	1000
12 <sup>b</sup>	Pd/Mordenite	H <sub>2</sub> , bubbling	7.5	1.0	64	85,000
13 <sup>c</sup>	Pd(OAc) <sub>2</sub>	As received	7.5	3.0	25	34,000
14 <sup>c</sup>	Pd(OAc) <sub>2</sub>	H <sub>2</sub> , bubbling	2.5	3.0	75	370,000

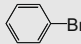
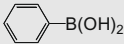
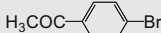
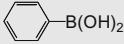
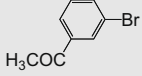
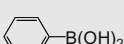
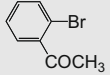
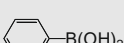
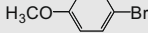
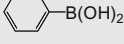
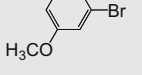
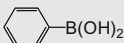
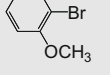
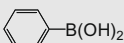
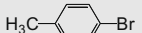
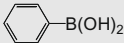
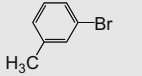
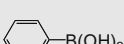
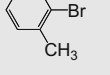
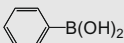
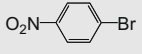
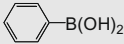
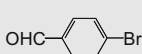
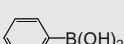


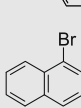

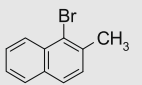
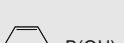
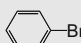
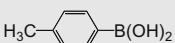



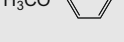
<sup>a</sup> Typical reaction conditions (Entries: 4, and 6): See footnote of Fig. 10.

<sup>b</sup> 0.4 wt%-Pd(NH<sub>3</sub>)<sub>4</sub>Cl<sub>2</sub> was loaded. The scales of all reagents were changed while the catalyst weight was fixed at 1.0 mg ( $3.8 \times 10^{-8}$  mol of Pd).

<sup>c</sup>  $3.8 \times 10^{-8}$  mol of Pd was used, in homogeneous phase.

**Table 3**  
Results of coupling reactions catalyzed by 0.4 wt%-Pd/USY activated with H<sub>2</sub> under in situ conditions<sup>a</sup>



Entry	Ar-Br	Ar'-B(OH) <sub>2</sub>	Pd/10 <sup>-4</sup> mol%	Time (h)	Yield (%)	TON
1			0.7	2.0	>99	1,300,000
2			0.2	0.7	99	5,300,000
3			0.4	2.0	>99	2,670,000
4			750	3.0	>99	1300
5			0.9	0.3	>99	1,060,000
6			2.5	1.0	88	120,000
7			1.9	3.0	74	870,000
8			0.9	1.5	98	1,040,000
9			0.9	1.5	38	280,000
10			0.9	1.0	82	880,000
11			0.9	0.8	>99	1,060,000
12			0.9	0.5	>99	1,060,000
13			7.5	1.0	>99	130,000
14			7.5	0.2	>99	130,000
15			7.5	1.0	83	120,000
16			1.5	1.0	86	590,000
17			7.5	3.0	84	120,000
18 <sup>b</sup>			75	8.0	>99	14,000

<sup>a</sup> Typical reaction conditions (Entry 1): see footnote of Fig. 10. The scales of all reagents were changed while the catalyst weight was fixed at 1.0 mg.

<sup>b</sup> At r.t.

poor activity. In particular, negligible activity was observed over PdCl<sub>2</sub>/USY even after the in situ activation (entry 4, TON = 0). Probably, the fact could be explained with the QXAFS data, where

growth of Pd clusters progressed immediately on exposure of PdCl<sub>2</sub>/USY to H<sub>2</sub> at r.t. to give large Pd particles (ca. 3 nm) as shown in Fig. 6. Thus, the importance of the selection of Pd precursors



**Table 4**

Results of coupling reactions catalyzed by 0.4 wt%-Pd-loaded USY catalysts prepared using different kinds of precursors<sup>a</sup>.

Entry	Precursor	Pd ( $10^{-4}$ mol%)	Time (h)	Yield (%)	TON
1 <sup>b</sup>	Pd(NH <sub>3</sub> ) <sub>4</sub> Cl <sub>2</sub>	0.4	2.0	64	1,700,000
2 <sup>b</sup>	Pd(NH <sub>3</sub> ) <sub>4</sub> (NO <sub>3</sub> ) <sub>2</sub>	0.4	2.0	64	1,700,000
3 <sup>c</sup>	Pd(OAc) <sub>2</sub>	0.7	3.0	25	340,000
4 <sup>c</sup>	PdCl <sub>2</sub>	0.7	3.0	0	0

<sup>a</sup> Catalyst (0.4 wt%-Pd/USY, 1.0 mg), 383 K, N<sub>2</sub> atmosphere.

<sup>b</sup> Bromobenzene (100 mmol), phenylboronic acid (160 mmol), K<sub>2</sub>CO<sub>3</sub> (200 mmol), *o*-xylene (280 mL).

<sup>c</sup> Bromobenzene (50 mmol), phenylboronic acid (80 mmol), K<sub>2</sub>CO<sub>3</sub> (100 mmol), *o*-xylene (140 mL).

could be recognized from the striking difference in activities given in Table 4.

### 3.7. Effect of the selection of bases and solvents for the reaction

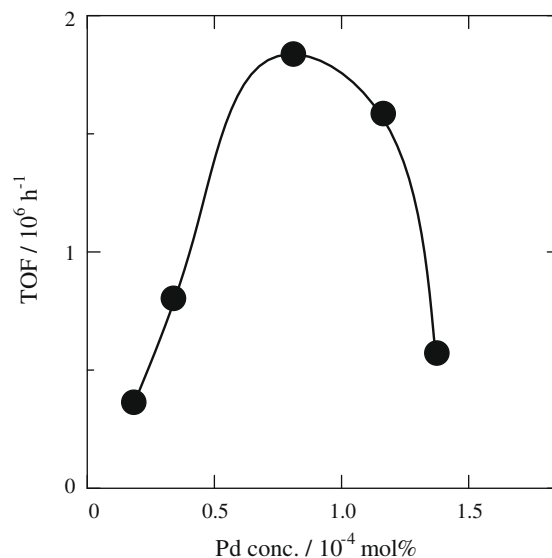
Table 5 shows the data of the reaction between bromobenzene and phenylboronic acid using various kinds of bases and solvents. The in situ-activated Pd/USY was employed as the catalyst. The very high activity was obtained only when *o*-xylene and potassium carbonate were used for the reaction as a solvent and a base, respectively. The effectiveness of the potassium carbonate agreed with the literature [20]. Although the reason for poor activity of the reactions using polar solvents such as H<sub>2</sub>O, H<sub>2</sub>O/DMF (1:1), and DMF was not clear at present, probably the reducibility of Pd was affected by the polar solvents. In this regard, additional QXAFS measurements for Pd/USY immersed in the solution are necessary since the XAFS data given here were collected in a gas flow.

### 3.8. Effect of the loading and the repetition times for reduction of Pd/USY

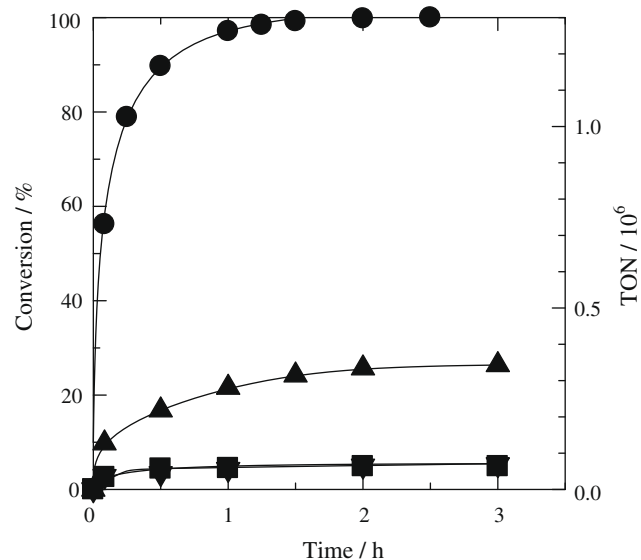
Fig. 11 shows the turn-over frequency (TOF) of the in situ-activated Pd/USY plotted as a function of the mol% of Pd with respect to the bromobenzene. The TOF of Pd was measured at the 0.5 h from the beginning of the reaction. The TOF showed a sharp dependence on the loading of Pd and the maximum TOF (1,800,000 h<sup>-1</sup>) was attained at the Pd concentration of  $8 \times 10^{-5}$  mol%.

Fig. 12 shows time course change in the conversion of bromobenzene over the Pd/USY catalysts that were repeatedly reduced with H<sub>2</sub>. The pre-treatment of Pd/USY was carried out through the alternative exposure of air and 6% H<sub>2</sub>. It could be seen that the activity tended to decrease accompanied by the repetition of oxidation–reduction treatments. The yield of product treated with H<sub>2</sub> for 4 times was identical to that of Pd/USY treated with H<sub>2</sub> for 3 times. The tendency was consistent with the QXAFS observations, in which the progressive growth of Pd clusters was observed through the repeated exposure of O<sub>2</sub> and H<sub>2</sub> as reported earlier (Fig. 1) [4].

In order to confirm the heterogeneous nature of the Pd/USY, the reaction between bromobenzene and phenylboronic acid was car-



**Fig. 11.** Dependence of the turn-over frequency of Pd on the concentration of Pd in the reaction between bromobenzene and phenylboronic acid. Catalyst: 0.10–0.74 wt%-Pd(NH<sub>3</sub>)<sub>4</sub>Cl<sub>2</sub>/USY. The samples were activated with bubbling H<sub>2</sub> at 300 K. Reaction conditions: bromobenzene (50 mmol), phenylboronic acid (80 mmol), catalyst (1.0 mg), K<sub>2</sub>CO<sub>3</sub> (100 mmol), *o*-xylene (140 mL), 383 K, N<sub>2</sub> atmosphere.



**Fig. 12.** Time course change of the conversion of bromobenzene in the reaction between bromobenzene and phenylboronic acid over 0.4 wt%-Pd(NH<sub>3</sub>)<sub>4</sub>Cl<sub>2</sub>/USY repeatedly activated with O<sub>2</sub>–H<sub>2</sub> by 1 (●), 2 (▲), 3 (■), 4 (▼) times. Reaction conditions: see the footnote of Fig. 10.

**Table 5**

Effect of the kinds of solvent and bases for the Suzuki–Miyaura reaction between bromobenzene and phenylboronic acid<sup>a</sup>.

Entry	Solvent	Base	Temp. (K)	Pd ( $10^{-4}$ mol%)	Time (h)	Yield (%)	TON
1	<i>o</i> -xylene	K <sub>2</sub> CO <sub>3</sub>	383	0.7	2.0	>99	1,300,000
2	DMF	K <sub>2</sub> CO <sub>3</sub>	383	7.5	2.0	10	13,000
3	H <sub>2</sub> O	K <sub>2</sub> CO <sub>3</sub>	373	7.5	1.0	9	13,000
4	DMF/H <sub>2</sub> O <sup>b</sup>	K <sub>2</sub> CO <sub>3</sub>	373	3.8	5.0	9	28,000
5	<i>o</i> -xylene	KF	383	7.5	4.0	51	70,000
6	<i>o</i> -xylene	K <sub>3</sub> PO <sub>4</sub>	383	7.5	4.0	97	130,000

<sup>a</sup> Catalyst (0.4 wt%-Pd/USY, 1.0 mg), N<sub>2</sub> atmosphere.

<sup>b</sup> Mixture of DMF and H<sub>2</sub>O (1:1).

ried out over the filtered solution; after the reaction using in situ-activated Pd/USY corresponding to entry 4 in Table 2, the solution was quickly filtrated while the temperature was maintained higher than 373 K to avoid the possibility of deposition of Pd (hot filtration) [32]. To the filtered solution, substrates (bromobenzene, phenylboronic acid, and  $K_2CO_3$ ) were newly added, followed by heating the solution to 383 K in the atmosphere of  $N_2$ . However, no further increase in the yield of product (biphenyl) was observed, meaning the reaction did not take place in the solution. Probably, the leaching of Pd was suppressed by using a non-polar solvent (*o*-xylene) instead of polar solvents such as DMF and  $H_2O$ .

#### 4. Conclusions

The combined studies using QXAFS technique and catalytic reactions were carried out. As a result, we found that the Pd clusters generated in the 0.4 wt%-Pd/USY zeolite worked very efficiently in Suzuki–Miyaura reactions. The ligand-free Pd cluster catalyst was prepared by the quite simple method that involved  $H_2$ -bubbling into a reaction solution containing 1.0 mg of 0.4 wt%-Pd/USY catalyst prior to the reaction. For the preparation of highly dispersed Pd clusters in this manner, the knowledge obtained by QXAFS technique was efficiently applied; Pd<sub>13</sub> clusters were generated through the exposure of  $H_2$  to the as-prepared Pd<sup>2+</sup>/USY at r.t. The use of Pd ammine complexes was essential to afford the finely dispersed clusters. We believe that the excellent nature of this catalyst will help in better understanding of the metal cluster catalysts prepared under in situ conditions.

#### References

- [1] M. Boudart, *J. Mol. Catal.* 30 (1985) 27.
- [2] L.N. Lewis, *Chem. Rev.* 93 (1993) 2693.
- [3] A. De Meijere, F. Diederich (Eds.), *Metal-Catalyzed Cross-Coupling Reactions*, second ed., Wiley-VCH, Weinheim, 2004, p. 31.
- [4] K. Okumura, T. Honma, S. Hirayama, T. Sanada, M. Niwa, *J. Phys. Chem. C* 112 (2008) 16740.
- [5] K. Okumura, J. Amano, N. Yasunobu, M. Niwa, *J. Phys. Chem. B* 104 (2000) 1050.
- [6] K. Okumura, R. Yoshimoto, T. Uruga, H. Tanida, K. Kato, S. Yokota, M. Niwa, *J. Phys. Chem. B* 108 (2004) 6250.
- [7] A. Suzuki, *J. Organomet. Chem.* 576 (1999) 147.
- [8] A. Suzuki, in: D. Astruc (Ed.), *Modern Arene Chemistry*, Wiley-VCH, Weinheim, 2002, p. 53.
- [9] J.H. Kirchhoff, C.Y. Dai, G.C. Fu, *Angew. Chem. Int. Ed.* 41 (2002) 1945.
- [10] J.E. Milne, S.L. Buchwald, *J. Am. Chem. Soc.* 126 (2004) 13028.
- [11] A.C. Hillier, G.A. Grasa, M.S. Viciu, H.M. Lee, C. Yang, S.P. Nolan, *J. Organomet. Chem.* 653 (2002) 69.
- [12] E. Peris, R.H. Crabtree, *Coordin. Chem. Rev.* 248 (2004) 2239.
- [13] R.B. Bedford, C.S.J. Cazin, D. Holder, *Coordin. Chem. Rev.* 248 (2004) 2283.
- [14] R. Chincilla, C. Nájera, M. Yus, *Chem. Rev.* 104 (2004) 2667.
- [15] N.E. Leadbeater, *Chem. Commun.* (2005) 2881.
- [16] M.T. Reetz, R. Breinbauer, K. Wanninger, *Tetrahedron Lett.* 37 (1996) 4499.
- [17] H. Sakurai, T. Tsukada, T. Hirao, *J. Org. Chem.* 67 (2002) 2721.
- [18] G. Cravotto, M. Beggiato, A. Penoni, G. Palmisano, S. Tollari, J.-M. Lévêque, W. Bonrath, *Tetrahedron Lett.* 46 (2005) 2267.
- [19] A. Corma, H. García, A. Leyva, *Appl. Catal. A* 236 (2002) 179.
- [20] G. Durgun, Ö. Aksin, L. Artok, *J. Mol. Catal. A* 278 (2007) 189.
- [21] B.M. Choudary, S. Madhi, N.S. Chowdari, *J. Am. Chem. Soc.* 124 (2002) 14127.
- [22] K. Shimizu, S. Koizumi, T. Hatamachi, H. Yoshida, S. Komai, T. Kodama, Y. Kitayama, *J. Catal.* 228 (2004) 141.
- [23] K. Mori, K. Yamaguchi, T. Hara, T. Mizugaki, K. Ebitani, K. Kaneda, *J. Am. Chem. Soc.* 124 (2002) 11572.
- [24] D.E. Bergbreiter, P.L. Osburn, A. Wilson, E.M. Sink, *J. Am. Chem. Soc.* 122 (2000) 9058.
- [25] Y. Yamada, Y. Maeda, Y. Uozumi, *Org. Lett.* 8 (2006) 4259.
- [26] K. Okitsu, A. Yue, S. Tanabe, H. Matsumoto, *Bull. Chem. Soc. Jpn.* 74 (2002) 449.
- [27] H. Bulut, L. Artok, S. Yilmaz, *Tetrahedron Lett.* 44 (2003) 289.
- [28] M. Dams, L. Drijkoningen, B. Pauwels, G. Van Tendeloo, D.E. De Vos, P.A. Jacobs, *J. Catal.* 209 (2002) 225.
- [29] L. Djakovitch, K. Köhler, *J. Mol. Catal. A* 142 (1999) 275.
- [30] J.B.A.D. van Zon, D.C. Koningsberger, H.F.J. van't Blik, D.E. Sayers, *J. Chem. Phys.* 82 (1985) 5742.
- [31] J.A. Gladysz, *Pure Appl. Chem.* 73 (2001) 1319.
- [32] Y. Ji, S. Jain, R.J. Davis, *J. Phys. Chem. B* 109 (2005) 17232.